Photocatalytic degradation of organic pollutants in water using graphene oxide composite

Suneel Kumar, [a] Chiaki Terashima,[b] Akira Fujishima, [b] Venkata Krishnan, [a]* Sudhagar Pitchaimuthu [c]*

[a] School of Basic Sciences and Advanced Materials Research Center, Indian Institute of Technology Mandi, Kamand, Mandi-175005, Himachal Pradesh, India.
E-mail: vkn@iitmandi.ac.in.
[b] Photocatalysis International Research Center, Tokyo University of Science,
2641 Yamazaki, Noda, Chiba 278-8510, Japan
[c] Multi-functional Photocatalyst & Coatings Group, SPECIFIC, College of Engineering, Swansea University (Bay Campus), Swansea SA1 8EN, Wales, United Kingdom.
Email: S.Pitchaimuthu@swansea.ac.uk.
(* Corresponding authors)

Abstract. Developing sustainable and less-expensive technique is always challenging task in water treatment process. This chapter explores the recent development of photocatalysis technique in organic pollutant removal from the water. Particularly, advantages of graphene oxide in promoting the catalytic performance of semiconductor, metal nanoparticle and polymer based photocatalyst materials. Owing to high internal surface area and rapid electron conducting property of graphene oxide fostering as backbone scaffold for effective hetero-photocatalyst loading, and rapid photo-charge separation enables effective degradation of pollutant. This chapter summaries the recent development of graphene oxide composite (metal oxide, metal nanoparticle, metal chalcogenides, and polymers) in semiconductor photocatalysis process towards environmental remediation application.

Keywords: Photocatalyst, graphene composite, organic pollutant degradation, advanced oxidation process.

1 Introduction

Clean and nonpolluted water is one of the basic requirements for all living organisms including human beings. But its availability is a major issue nowadays. In the future, this issue will further increase due to global industrialization and population growth. Natural water is being contaminated by the discharge of industrial, domestic, and agricultural wastes. Therefore, it is very important to remove the pollutants and pathogens from wastewater to fulfill the needs for irrigation as well

as industrial and domestic use. In the past years, conventional biological and physical treatment methods (adsorption, ultrafiltration, coagulation, etc.) have been used to remove the organic pollutants. These methods are still adequate in removing lower concentration of organic pollutant from the water. Also, it requires sophisticated techniques to convert chemically toxic pollutants into environmental benign species. *Non-renewable energy* based water treatment technologies are currently formulated for organic pollutant removal from industrial waste, which are driven by oil, electricity and chemical processes. The depletion of fossil fuel resources and emission of undesired by-products (CO_2) into the environment challenges the sustainability of these technologies.

In this context, advanced oxidation processes (AOPs) are more efficient, cheap, and eco-friendly in the degradation of any kind of toxic pollutants.[1] AOPs generate hydroxyl radical, a strong oxidant, which can completely degrade or mineralize the pollutants nonselectively into harmless products.[2] In detail, hydroxyl radical (OH·) is the most reactive oxidizing agent in water treatment, and can be operated under broad range of applied potential window. For instance, the operating potential at pH 0 is about 2.8 V vs SCE (saturated calomel electrode) and for pH 14 is 1.95 V vs SCE. Furthermore OH· is nonselective and rapid (rate constant $=10^8$–10^{10} M^{-1} s^{-1}) in oxidization of numerous organic species.[2] Hydroxyl radicals can react with organic pollutants through following routes: (a) radical addition, (b) hydrogen abstraction, (c) electron transfer, and (d) radical combination. While, organic compounds interact with hydroxyl radicals produce carbon-centered radicals (R· or R·–OH), and organic peroxyl radicals (ROO·). These radicals further react with organic pollutant and forming more reactive species such as H_2O_2 and super oxide ($O_2^{\bullet-}$) lead chemical degradation and mineralization. Due to extremely short life time, hydroxyl radicals are only in situ produced during application through different process.

Recently 'photocatalysis' based environmental remediation using oxide semiconductors perceived great deal of attention compare to other AOP's techniques.[3-5] Because, it can be functioned without external applied potential. The light irradiation on semiconductor catalyst is a key source (UV light, solar light, visible light sources, etc) to drive the catalysis reaction. This technique had long before received considerable study from the perspective of the *electronic theory of chemical catalysis*. For the last one decade, a huge quantity of research has been progressed in this area, and historically it dates back at least to the 1960s.[6] In the early studies, zinc oxide was a popular choice for the oxide semiconductor candidate. In 1979, Oliver et al reported the influence of *sunlight and rocks on natural remediation processes*.[7] Followed this work few research work has been reported on photocatalysis based water treatment.[7-9] Though these articles are pioneer in photocatalysis based environmental remediation, a ground-breaking phenomena *Fujishima– Honda* discovery[10] at 1972 could offer an explanation on how the combination of sunlight and semiconductor involved in water oxidation process. Here, photoelectrocatalytic process, the generation of photocharge carriers' electron (e^-) and holes (h^+) at a light irradiated semiconductor drive the catalysis reaction that facilitates the conversion of light energy into stored chemical energy. In analogous to photoelectrocatalytic water oxidation (**Figure 1a**), the photoholes

generated from valance band of semiconductor drives the pollutant oxidation or degradation of ambiguous refractory organic species into biodegradable compounds, and eventually mineralizing them to carbon dioxide and water. Though huge quantity of semiconductor photocatalyst materials are demonstrated in environmental remediation, yet photocatalysis reaction rate, selectivity and material stability were to be improved. In this view, graphene and graphene oxide derivatives can be applied in photocatalyst and it opens new avenue on composite based semiconductor photocatalyst. This chapter summarises the recent development of graphene oxide composite (metal oxide, metal nanoparticle, metal chalcogenides, and polymers) in semiconductor photocatalysis process towards environmental remediation application.

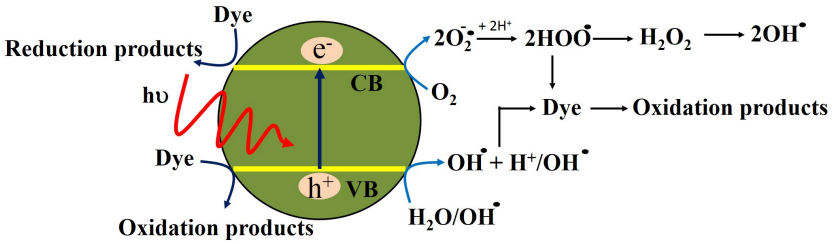

Figure 1. Schematic illustration of photocatalytic dye degradation using light and semiconductor (this scheme is redrawn based on Ajmal et al.[11] work)

2 Theory

2.1 Why graphene oxide composite in photocatalysis reaction?

The photocatalytic degradation of organic pollutants from water has gathered a great deal of interest as it utilizes renewable solar energy and produces non-toxic by-products during the reaction. On this note, several semiconductor materials including ZnO, SnO_2, WO_3, a-Fe_2O_3, and TiO_2 have been widely investigated (**Figure 2**). On the other hand, engineering the photocatalyst surface area also significantly influences the PC efficiency, as the degradation of organic pollutants takes place mostly at the semiconductor surface. Therefore, nanomaterials with very high surface area are considered to be effective for PC applications over micron-size materials. The nanostructured electrodes provide more adsorption sites for organic pollutants owing to their larger surface area. Among different nanostructures, two-dimensional (2D) nanostructures offer more effective channels for electron transport due to the reduced junctions and grain boundaries compared to spherical nanocrystals. Such fast electron transport decreases the rate of and enhance PC degradation performance. In this line, 2-D structured graphene oxide are appropriate candidate to promote the semiconductor photocatalysis performance.

In recent years, the potential applications of graphene oxide (GO)-semiconductors nanocomposites have been extensively investigated as heteroge-

neous catalysts due to fascinating electronic and optical properties of GO.[12, 13] Currently, the role of GO based nanocomposites for mineralization of various kinds of organic pollutants is one of the hot research fields worldwide.[14] As discussed above, owing to 2-D structure of GO, it possess high specific area with plenty of active sites, which facilitates the surface photocatalytic reactions.[14] Therefore, GO acts as one of superior support material to various semiconductors and metals to form effective heterojunction with enhanced photocatalytic performance.[15] From **Figure 2**, the TiO_2 nanoparticle decorated graphene oxide (GO), the photoelectrons generated at conduction band of TiO_2 is rapidly transferred to graphene layer which promote the organic dye pollutant degradation rate. Moreover, the high surface area of GO provides more surface adsorption sites for pollutants during photocatalytic reactions to significantly facilitate the surface photocatalytic reactions, thereby enhancing the catalytic activity.[15] It is noteworthy to mention that, GO gets always reduced to graphene or reduced GO during synthesis of nanocomposites to revive the conjugation and high conductivity.[16] In photocatalytic reactions, graphene acts as an excellent electron sink to capture and shuttle the electrons due to its ultra-high electron conductivity (200,000 $cm^2\ V^{-1}\ S^{-1}$).[17] Hence, graphene effectively retards the electron-hole recombination in semiconductors, which is one of the key steps in photocatalytic reactions.[18] Furthermore, the Fermi level of graphene (0 V vs NHE) is less negative than most of the semiconductor materials, which results in the favorable band gap alignment of semiconductors and graphene.[17] It is well known that, electrons transfer takes place 'down potential' while holes transfer lead 'up potential', hence in nanocomposites the electrons transfer occurs from conduction band (CB) of semiconductors to graphene and active species radical's formation take place, which results in the degradation of organic pollutants.[16]

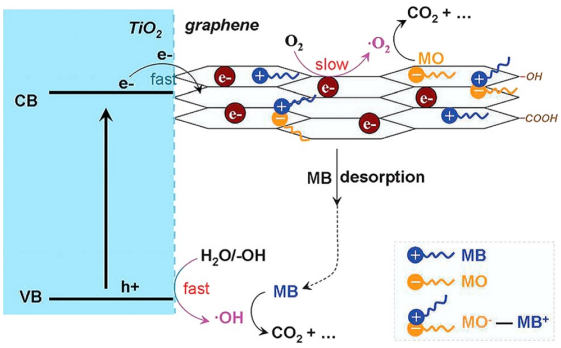

Figure 2. Photocatalysis based organic dye pollutant removal using TiO_2-graphene oxide composite. Reprinted with permission from reference [19], copyright 2013 American Chemical Society.

3 Semiconductor-graphene oxide nanocomposites

3.1. Metal oxide-graphene oxide nanocomposites

Among semiconductor oxides, TiO_2 and ZnO are widely explored in photocatalytic pollutants removal due to their appropriate band gap energy, non-toxic nature and earth abundance.[20, 21] Recently, Jiang et al. [22] reported the graphene oxide-TiO_2 nanocomposite (GO-TiO_2) synthesis route using liquid phase deposition method. In this method, TiO_2 nanoparticles were grown *in-situ* over 2-D GO nanosheets. The photocatalytic activity of this nanocomposite has been demonstrated for the degradation of methyl orange dye and reductive conversion of toxic, inorganic pollutant Cr(VI) to non-toxic Cr(III). The as prepared GO-TiO_2 nanocomposite exhibit several times higher activity than bare catalysts and P25 (commercial TiO_2) due to high surface area of nanocomposite (80 m^2 g^{-1}), more pollutants adsorption ability and fast charge transfer. Moreover, due to the high work function of GO, the photoexcited electrons form CB of TiO_2 are easily transferred to GO, which suppresses their recombination. Thus, the transferred photoinduced electrons participate in the oxidative degradation of organic dyes and reductive conversion Cr(VI) to Cr(III), which leads to enhanced photocatalytic activity of nanocomposite. In addition to these two pollutants, the prepared graphene oxide-TiO_2 nanocomposite was also applied for degradation of other azo dyes such as methyl red, orange G, acid orange 7 and notably improved performance was observed.

The GO based nanocomposites have also shown their potential for the degradation of volatile aromatic pollutants in air along with their removal from water and is widely reported in literature. In this regard, Zhang et al. [23] reported graphene-TiO_2 nanocomposite by hydrothermal reduction of GO. They varied the amount of graphene in nanocomposite and investigated the comparative photocatalytic activity of various compositions for removal of methylene blue from water and benzene, a volatile aromatic pollutant, in air. Interestingly, it was observed that the nanocomposites with higher amount of graphene exhibit decreased activity towards pollutants removal, which is analogous with liquid-phase degradation of organic pollutants. The graphene being a zero-band gap semiconductor exhibit absorption in entire solar spectrum. Thus, the improved photocatalytic performance of graphene-TiO_2 nanocomposite has been attributed to the extended solar energy utilization, fast charge transfer which results in the formation of highly reactive $^*OH$ which results in the mineralization of benzene/organic dyes into CO_2 and H_2O.

In addition to TiO_2, numerous studies have been carried out on other semiconductors oxides-GO nanocomposites for environmental remediation applications. In 2009, a very interesting study by Li et al. [24] proved ZnO as better photocatalytic material than TiO_2 because of high efficiency of photoinduced charge generation and prolonged lifetime of charge carriers. This report has stimulated extensive research work on the fabrication of ZnO and GO based nanocomposite materials as efficient photocatalysts for the removal of various organic pollutants from water. Very recently, Bai et al. [25] reported the hydrothermal synthesis of graphene-ZnO

nanocomposites and demonstrated it for mycotoxin detoxification by degrading deoxynivalenol (DON) from water under UV light irradiation. DON is one of several mycotoxins produced by certain Fusarium species that frequently infect corn, wheat, oats, barley, rice, and other grains in the field or during storage which can possess a serious threat to water environment. ZnO is photo-excited by UV irradiation and once in hybridization with graphene, the photocatalytic activity of nanocomposite is substantially enhanced as compared to pure ZnO. Graphene accelerates photocatalytic process by suppressing photogenerated electron-hole recombination and adsorption of pollutants as presented in **Figure 3**. **Figure 3 (a)** describes the synergetic effect between graphene and ZnO wherein, photogenerated electrons transfer takes place form CB of ZnO to graphene to degrade the adsorbed pollutant by generating active species. The active species trapping experiments reveals that superoxide radicals (O_2^{-*}) and holes (h^+) were active species formed during the photocatalytic reaction. **Figure 3 (b)** shows the adsorption effect more dominating with the increasing amount of graphene in nanocomposite but at same time higher amount of graphene leads to the decrease in the photocatalytic activity due to the shading effect, which hinders ZnO to absorb light energy and hence there is lesser generation of charge carriers, which decreases photocatalytic performance. It observed that nanocomposite with 0.3 wt% of graphene shows highest photocatalytic performance. Therefore, it implies that the trade-off between charge generation (synergetic effect) and light harvesting (competitive effect) leads to improved photocatalytic activity with the optimized amount of graphene, which possesses excellent adsorption. The optimized photocatalyst with 0.3 wt% of graphene degraded about 99% of DON (15 ppm) in 30 min under UV irradiation.

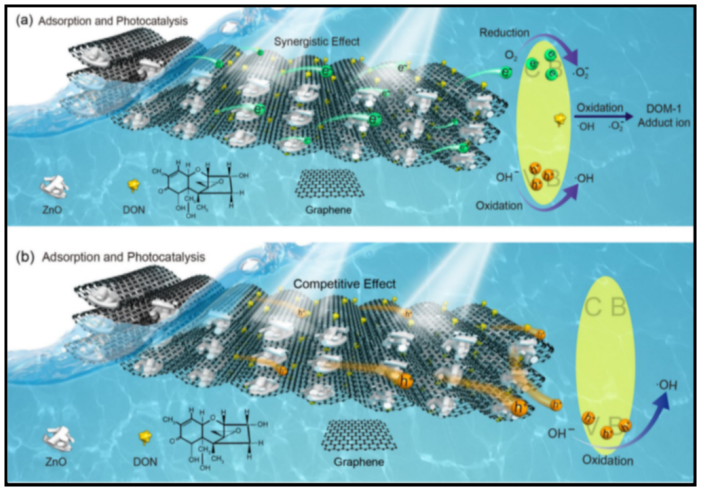

Figure 3. Charge separation, transfer mechanism and adsorption-photocatalytic process over graphene-ZnO photocatalysts under UV light irradiation. Reprinted with permission from reference [25], copyright 2016 Elsevier.

3.1.2. Metal chalcogenide-graphene oxide nanocomposites

For the past one decade, two dimensional materials has attracted immense attention of the scientists working in the field of nanomaterials due to their interesting electronic properties, which has lead research into device fabrication for diverse technological applications.[26] In this regard, transition metal dichalcogenides which are semiconductors of type MX_2 where M is transition metal, such as Mo or W, and X is chalcogen atom (O, S, Se and Te) have been widely explored due to atomically thin nature of nanosheets with abundant reaction sites, for various applications, including pollutants removals.[27] Furthermore, semiconductors like MoS_2 has narrow band gap of ~1.86 eV, which allows the harvesting of visible light energy.[28] However, the narrow band gap of materials like MoS_2 results in high recombination rate of the photogenerated charge carriers and hence limits their use in potential applications.[28] Therefore, a single material cannot possess all the properties to accomplish the photocatalytic activity. The nanocomposite formation of MoS_2 with materials like GO could be one of the promising strategies and can offer several potential merits to nanocomposites. Firstly, better utilization of solar energy spectrum, as semiconductors with narrow band gaps possess high light absorption efficiencies. Secondly, efficient charge separation and its transportation to active reaction sites on the catalyst surface to boost the photocatalytic activity. In consideration of the above facts, Ding et al. [29] reported MoS_2-graphene oxide (GO) nanocomposite by one step hydrothermal hydrogel method with significantly enhanced solar light absorption and photocatalytic activity towards the degradation of methylene blue, a dye pollutant. About 99% of dye was degraded in 60 min of solar light irradiation with optimized nanocomposite having 10 wt% of MoS_2. The improved charge transfer mechanism of nanocomposite has been supported by electron impedance spectroscopy (EIS) analysis. Similar MoS_2-reduced graphene oxide (RGO) nanocomposite has been fabricated by Zhang et al. [30] by simple hydrothermal synthesis method. This prepared nanocomposite exhibits effective separation of photogenerated charge carriers and has been supported by photoluminescence measurements, which reveals minimum recombination of photogenerated charge carriers. Upon visible light irradiation, electron-hole pair formation takes place and electrons form CB of MoS_2 gets transferred to RGO resulting in the degradation of RhB dye by the formation of superoxide radicals (O_2^{-*}) as active oxidizing species. Thus, the formation of hetero-interface between MoS_2 and RGO results in the separation of photogenerated charge carriers and suppresses their recombination, which is responsible for enhanced photocatalytic activity under visible light irradiation for pollutant removal.

Very recently, micron thin, flexible paper morphology of MoS_2–RGO hybrid layers has been synthesized and demonstrated for photocatalytic degradation of organic dyes by Jeffery et al. [31]. The potential of macrostructure, self-standing film has been shown in this work for environmental cleanup. For the preparation of such unique hybrid, a simple exfoliation method involving evapora-

tion under ambient conditions has been demonstrated. Such kind of 2D-2D nanocomposites are formed by co-stacking of different layers with large face-to-face contact area, which allows more electronic interactions between the two 2D components. Therefore, 2D-2D composites exhibit improved activity due to more pollutant adsorption and excellent charge separation at interfacial regions. This nanocomposite was also proved to be active for the photocatalytic reduction reactions of nitro compounds to amino compounds, which has some medical significance.

In addition to dichalcogenides, metal sulfides such as cadmium sulfide (CdS) and zinc sulfide (ZnS) are of great research interest due to their potential applications for pollutant removals.[32] CdS is one of fascinating II-VI semiconductor materials with direct band gap energy of ~ 2.4 eV, which makes it active under visible light.[32] The CB potential and VB potential of CdS are -0.52 V and 1.88 V, respectively indicates the strong reducing power of electrons, which is highly beneficial for photocatalytic reactions.[33] Therefore, CdS has been widely explored for various applications, including pollutants removal.[33] But pure CdS suffers from various limitations, such as fast charge recombination, poor pollutant adsorption capacity and low photostability, which restrict its practical applications. Thus, construction of nanocomposite of CdS with materials like GO can bring about the effective charge separation and transfer of photogenerated charge carriers because of less negative Fermi energy level. Chen et al.[34] synthesized nanocomposite comprising of CdS nanospheres decorated over reduced graphene oxide (RGO) sheets by facile hydrothermal synthesis process. The interfacial contact between CdS nanospheres and RGO acts as bridge for fast transfer to photogenerated charge carriers, as presented schematically in **Figure 4 (a)**. Whereas, **Figure 4 (b)** presents the TEM images of CdS-RGO nanocomposite showing homogenous CdS nanospheres well dispersed over RGO nanosheeets to form the intimate interfacial contact between them. These nanocomposites with different loading of RGO were demonstrated to be very effective for selective reduction of nitro-aromatic compounds to amino compounds in aqueous phase. The nanocomposite with 5% of RGO exhibits the highest photocatalytic performance for 4-nitroaniline reduction. The excellent pollutant adsorption ability of RGO and improved photogenerated charge separation gives opportunity for the transferred electrons to reduce the adsorbed species.

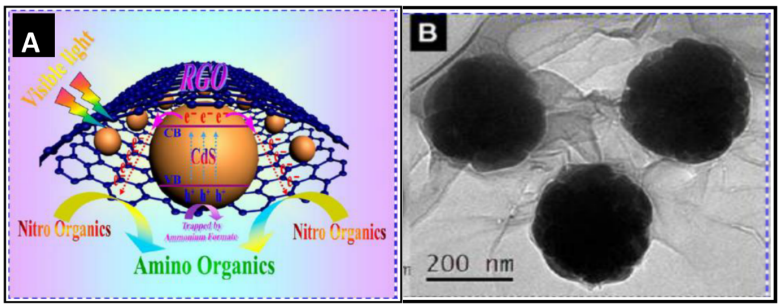

Figure 4. (A) Schematic diagram of photocatalytic reduction of nitrocompounds over the surface of CdS-RGO catalyst, (B) TEM images of CdS nanospehers on

RGO nanosheets. Reprinted with permission from reference [34], copyright 2013 American Chemical Society.

3.1.3. Carbon quantum dot-graphene oxide nanocomposites

The fluorescent carbon nanoparticles or carbon quantum dots (CQD) have gained much importance recently because of their fascinating electronic, optical and physicochemical properties,.[35] The low toxicity, environmental benignity, cost effectiveness, biocompatibility and facile synthesis routes of CQD makes them promising material for diverse technological applications, including the field of photocatalysis.[35] The physicochemical properties of CQD can be tuned by surface functionalization with enhanced fluorescence emission.[36] These carbon nanomaterials were discovered in 2004 by Xu et al.,[37] during purification of single-walled carbon nanotubes through electrophoresis, provides a pathway to new class of fluorescent materials. Sun et al.,[38] in 2006 reported these fluorescent carbon nanoparticles by surface passivation with much enhanced fluorescence emission properties and named them as carbon quantum dots (CQD). CQD are usually prepared by laser ablation of graphite, electrochemical oxidation of graphite, electrochemical soaking of carbon nanotubes, thermal oxidation of suitable molecular precursors, vapor deposition of soot, proton-beam irradiation of nano diamonds, microwave synthesis and bottom-up methods.[35] The CQD are advantageous over several of semiconductors based quantum dots, because of their facile surface passivation to enhance emission fluorescence, their benign chemical composition, easy surface functionalization and high resistance to photobleaching.[35] Moreover, semiconductors based quantum dots involves the use of heavy metal ions in their preparation, which are highly toxic even in low concentration.[35] CQD are conjugated materials with quasi spherical structure comprising of crystalline to amorphous sp^2 hybridized carbon atoms. It is noteworthy to mention here that, the photoluminescence of CQD can be quenched efficiently by either electron acceptor or electron donor molecules in solution, which reveals their excellent electron donor and electron acceptor behavior.[36] These desired properties of CQD can be exploited for technological applications such as photocatalysis, energy storage devices and sensing.[35] In addition, CQD exhibit upconversion photoluminescence property, which makes them even more desirable material for photocatalysis applications, especially to make use of the larger infrared region of the solar spectrum. It has been reported that, CQD exhibit emission in visible region when excited by the femtosecond pulsed laser in near infrared range (NIR).[36] The size dependent photoluminescence and excellent upconversion photoluminescence properties of CQD have been investigated in detail by excitation wavelength in range of 500-1000 nm with upconversion emission bands in 325-425 nm range. Therefore numerous studies have been devoted and significant advancement has been achieved to fabricate CQD-semiconductor based nanocomposite to exploit the maximum region of solar energy spectrum and investigate them for photocatalytic water purification by removing various kind of organic pollutants. In this regard, Li et al. [36] designed photocatalysts of CQD-TiO_2 and CQD-SiO_2 by alkali assisted electrochemical synthesis route to harvest the full solar energy spectrum. The nanocomposite formation of CQD and semiconductors with intimate interfacial contact has

been confirmed by scanning electron microscopy (SEM) and high resolution transmission electron microscopy (HRTEM) presented in **Figure 5 (a, b)**. On light irradiation to CQD-TiO_2 and CQD-SiO_2 photocatalyst, the CQD absorb visible light, and then emit light in UV region due to upconversion property. This upconverted light energy can excite TiO_2 or SiO_2 semiconductors to form electron-hole pairs (**Figure 5c**). Furthermore, the nanocomposite formation between semiconductors and CQD favors the electrons transfer from their CB to CQD as per suitable band gap potentials. Thus, photogenerated charge carriers are transferred rapidly through highly conducting CQD on catalyst surface to enhance the photocatalytic performance of the nanocomposites. These photogenerated charge carriers produce active oxygen species mainly O_2^{-*}, OH^* in aqueous photocatalytic reaction mixture with dissolved O_2, which are highly oxidizing in nature and causes the mineralization of pollutants into CO_2 and H_2O.

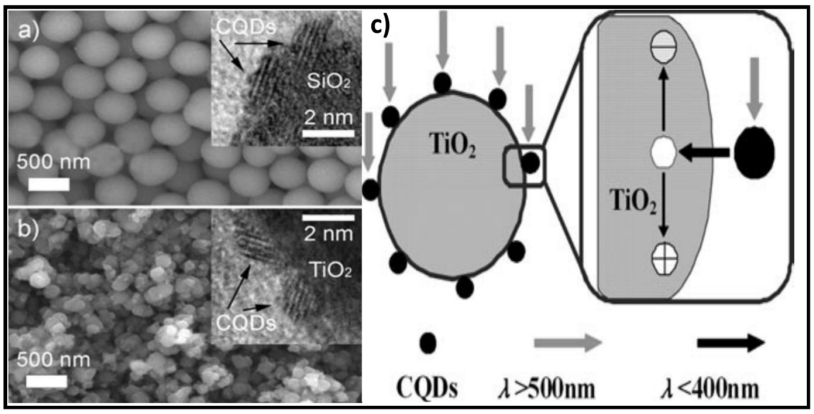

Figure 5. (a, b) SEM and HRTEM (Insets) images of CQD-SiO_2 and CQD-TiO_2 nanocomposite, (c) photocatalytic charge separation in TiO_2 by upconverted light from CQD. Reprinted with permission from reference [36], copyright 2010 Wiley-VCH.

Subsequently, Zhang et al. [39] reported the facile fabrication of CQD-Ag_3PO_4 and CQD-Ag-Ag_3PO_4 nanocomposites and demonstrated them as superior photocatalysts for the degradation of organic pollutants by harvesting visible light. The dual functionality of CQD has been discussed in detail to enhance photocatalytic performance, by facilitated charge transfer and to protect the Ag_3PO_4 form photocorrosion. The CQD acts both as, electron acceptor and donor, wherein electrons can be transferred to the surface of Ag_3PO_4 for photocatalytic reaction and redundant electrons can be transferred back to CQD. Moreover, the CQD layer on the surface of Ag_3PO_4 and Ag-Ag_3PO_4 particles can effectively protect Ag_3PO_4 from dissolution in aqueous solution. The up-conversion photoluminescence behavior of CQD utilizes the wide range of solar energy spectrum. As compared to pure Ag_3PO_4 and Ag-Ag_3PO_4, the CQD-Ag-Ag_3PO_4 exhibit higher photocatalytic performance and degrades methyl orange (MO) dye in 10 min of visible light irradiation. The PL spectra of CQD reveal the presence of emission

intensity peaks in 300-700 nm range when it was excited at higher wavelengths as 700-1000 nm. Hence this upconverted light excites Ag_3PO_4 which is one the narrow band gap (2.4 eV) semiconductor and results in the formation of photogenerated charge carriers. To confirm the role of upconverted light, the photocatalytic activity of Ag_3PO_4 and Ag-Ag_3PO_4 was checked by the researchers, under NIR light and almost negligible degradation was observed, while CQD-Ag_3PO_4 and CQD-Ag-Ag_3PO_4 exhibit good photocatalytic activity under NIR irradiation. Furthermore, in case of the CQD-Ag-Ag_3PO_4 photocatalyst, the surface plasmon resonance (SPR) of Ag particles (intense electric fields at the Ag particle surface) can further increase electron-hole pair's generation on the surface Ag_3PO_4 particles.

Furthermore, Yu et al.,[40] reported the nanocomposite of CQD with mesoporous hematite (α-Fe_2O_3) by solvothermal process as efficient, recyclable photocatalyst for the degradation of organic compounds. Pure α-Fe_2O_3 possesses low activity due to poor conductivity and fast recombination of photogenerated charge carriers. α-Fe_2O_3 is an n-type semiconductor with narrow band gap (2.1 eV), and is the most thermodynamically stable phase of iron oxide. It has been well explored in the field of photocatalysis due to its non-toxicity, facile synthesis and high photostability. The mesoporous α-Fe_2O_3 has high surface area to volume ratio and the well-defined nanoporous skeleton structure contributes for the its improved photocatalytic activity. The α-Fe_2O_3-CQD nanocomposites exhibit improved charge transfer from the photoexcited α-Fe_2O_3 to highly conducting CQD framework, which enhances the MB dye degradation by harvesting visible light. The improved photocatalytic activity of α-Fe_2O_3 was attributed first to the high surface area (187 m^2g^{-1}) of α-Fe_2O_3-CQD nanocomposite with abundant reaction sites for pollutant adsorption and photocatalytic reaction. Secondly, the excellent catalytic dispersion results in fast photogenerated charge transfer to generate reactive oxidative species (O_2^{-*}, OH^*), which degrades the pollutants.

3.1.4. Metal nanoparticles-graphene oxide nanocomposites

It is well known that, metal nanoparticles, such as Au, Ag, Pt, Pd, and Ru exhibit interesting electronic, optical, and magnetic properties [41]. When light is incident on noble metals (Au, Ag, etc.), the oscillating electric field of light interacts with conduction electrons and resonance happens between the incident photon frequency and oscillating frequency of the conduction electrons, which results in resonance. This resonance is known as surface Plasmon resonance (SPR) and noble hence noble metals exhibit absorption in the visible region. Furthermore, the localized SPR of metal nanoparticles, mainly Au or Ag enables to tune their absorption bands in the visible light region.[42] Hence, noble metal nanoparticles based nanocomposites can be exploited as very efficient visible light active photocatalyst materials for pollutants removal. The nanocomposite formation of noble metal nanoparticles with GO is one of the promising strategy to retard the surface recombination of photogenerated charge carriers, wherein the charge transfer takes place from one component to another in photocatalytic reaction. By varying some parameters, such as size, shape, chemical composition and dielectric environment, the absorption properties of noble metal based nanocomposites can be tuned. This has stimulated extensive morphology based research on noble metal nanostruc-

tures. Various kinds of morphology investigated includes nanowires, nanorods, nanoprisms, nanoplates, polyhedral structures, etc.[43-46] Furthermore, the synthesis of nanoparticles with exposed high-energy or active facets has attracted considerable attention as well, because they usually exhibit fascinating interfacial behavior and have been applied in technological applications. [47, 48] Most of the conventional methods of loading of metal nanoparticles over GO surface includes the use of some reducing agents such as surfactants and polymers, which have the limitation of impurity in crystal lattice of the final nanocomposite. [49] Recently, Quin et al. [45] have successfully synthesized size specific Au nanoparticles decorated over GO sheets via facile hydrothermal reduction and crystallization method. Hence this was one of the major breakthroughs in the development of reducing agent free pathway to grow Au nanocrystals over GO sheets. The morphology of Au nanocrystals can be tuned by varying the degree of oxidation on GO surface.

Ullah et al.[50] have reported the one pot microwave assisted synthesis of Pt-graphene nanocomposite for photocatalytic degradation of organic dye pollutants RhB and MB by utilizing visible light energy. The uniform distribution of homogenous Pt nanoparticles over graphene sheets has been confirmed by transmission electron microscopy (TEM) images wherein intimate contact between both the constituents can be seen, which is highly advantageous to boost the photocatalytic activity of the nanocomposite (**Figure 6**). On visible light irradiation, the electrons are photoexcited from ground state to graphene, which acts as excellent electrons acceptor and transporter. Thus, the photoelectrons are transferred to Pt due to ultra-high charge carrier mobility of graphene. Hence efficient charge transfer takes at metal-graphene interface, which further forms superoxide radicals (O_2^{-*}) by reacting with dissolved oxygen and hydroxyl radicals (OH^*) from water. Both of these radical species are highly oxidizing in nature and results in the mineralization of dyes into CO_2 and H_2O.

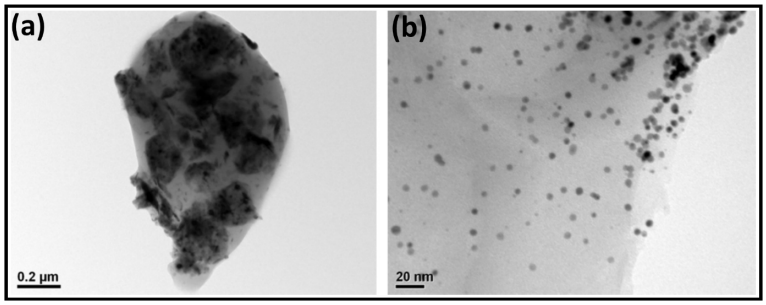

Figure 6. (a) Low magnification TEM image of Pt-graphene composite, (b) High magnification TEM image presenting graphene sheet decorated with Pt nanoparticles. Reprinted with permission from reference [50], copyright 2013 Elsevier.

Recently, Vilian et al. [51] reported Pd nanoparticles decorated on reduced graphene oxide (RGO) by using gum arabic solution as reducing agent. The in-situ synthesized Pd nanoparticles (5 nm) were found to be uniformly dispersed on RGO nanosheets and was employed as highly efficient catalyst for photocatalytic reduction of 4-nitrophenol (4-NP) pollutant to 4-amino phenol (4-AP) and its

sensing. 4-NP and its derivatives have been found to be highly toxic and carcinogenic to human beings. Hence their reduction by Green, sustainable technology and sensing is of great significance. The RGO support facilitates the charge transfer process in nanocomposites and increases the photocatalytic efficiency of reaction.

In the recent years, tremendous research efforts have been devoted to explore the bimetallic alloys (Pt-Au, Au-Ag, Au-Pd) for pollutants degradation reactions because of extended light absorption range and increased charge transfer processes.[52-54] Moreover, bimetallic systems offer more tunable parameters, synergistic effects and non-uniform charge distribution as compared to monometallic system, which can significantly enhance their photocatalytic activity for pollutants removal.[52] Moreover, coupling of such metallic alloys with GO can greatly enhance the charge transfer process in nanocomposite to boost their photocatalytic performance. Such bimetallic nanoalloys system composed of Au-Pd has been reported by Zhang et al. [54] supported over 2D reduced graphene oxide (RGO) in aqueous phase by one pot synthesis method. Herein, they reported the formation of stabilizer free Au-Pd-RGO nanocomposite in which RGO plays the role of surfactant and support material to nanoalloys. The reduction of precursor materials to form bimetallic alloys and loading over RGO occurs simultaneously. 2D RGO acts as an excellent support platform and a unique macromolecular surfactant to promote the formation of nanocomposite of bimetallic alloys with RGO. This report gives new insight on the role GO as surfactant due to presence of large number oxygenated defects and its reduction to RGO makes it more hydrophobic in nature. The photocatalytic performance of Au-Pd-RGO nanocomposite was demonstrated for the degradation of model pollutant rhodamine B under visible light irradiation. It was very interesting to note that, the photocatalytic activity of bimetallic alloy was found to be higher than both the monometallic systems (Au-RGO and Pd-RGO), which indicate the prolonged lifetime of charge carriers and their fast transfer in bimetallic system leading to their enhanced photocatalytic activity as compared to their respective monometallic counterparts.

Furthermore, the physicochemical properties of noble metals have been exploited for catalysis applications. In order to enhance the catalytic performance, the carbon material mainly GO support plays crucial role by boosting the charge transfer process in nanocomposites. Therefore, owing to their advantages, Ye et al. [55] recently reported the Green synthesis of Pt-Au dendrimer alloy supported over the surface of functionalized RGO. Thus Pt-Au exhibit dendrimer type morphology composed of nanoparticles and exhibit abundant edge sites and corner atoms, which can significantly enhance the catalytic performance. The surface of RGO was functionalized with polydopamine (PDA), which polymerizes by self-polymerization of dopamine and acts as reducing agent to graphene oxide (GO). PDA is biocompatible and stable polymer and hence, the use of toxic reducing agents such as hydrazine or sodium boron hydride could be avoided for reduction of GO to RGO and hence environmental benign route was adopted for synthesis. The various functional groups of PDA, such as amine and catechol, play a crucial role in the stabilization of metal nanoparticles by electrostatic interactions with their negatively charged precursor ions. The catalytic activity of Pt-Au alloy sup-

ported over PDA-RGO was tested for reduction of 4-NP to 4-AP. The loading effect of Pt to Au ratio has been systematically studied and the nanocomposite having 3:1 ratio was found to exhibit enhanced catalytic performance for reduction of 4-NP. Moreover, control experiments with PDA-RGO as catalyst reveal the strong adsorption of pollutant, which diminishes the absorption intensity of characteristic peak of 4-NP around 400 nm but no peak at 300 nm (4-AP) was detected. While in case of nanocomposites with Pt-Au alloy supported PDA-RGO surface, the decrease in absorption peak intensity at 400 nm occurs simultaneously with the appearance of peak at 300 nm, which corresponds to reduced product of 4-NP. The enhanced activity of optimized nanocomposite as compared to Pt-PDA-RGO, Au-PDA-RGO and Pt/C (commercial catalyst) has been attributed to the high electron density on the alloy due to PDA followed by electron transfer from Au to Pt, which facilitates the transfer to adsorbed 4-phenolate ions to reduce them.

3.1.5. Polymer-graphene oxide nanocomposites

Polymer-GO nanocomposites have been identified as one of the promising materials for water purification by removal of pollutants. Therefore, research in this area has also been emphasized by scientific community due to their sustainability and environmental benignity, which has opened new paths for materials with improved physicochemical properties.[56] The investigation on polymers-graphene nanocomposites for environmental remediation applications is one of the key additions in this field of materials science and technology.[56] Polymer-graphene nanocomposites are fabricated by dispersing exfoliated graphene into polymer matrix, which leads to interesting properties different form bare polymers. There are several reports available in literature on polymer-graphene nanocomposite such as epoxy,[57] PMMA,[58] polypropylene,[59] polystyrene,[60] Nylon,[61] polyaniline,[62] and silicone rubber,[63]. These reports have investigated that hybridization of graphene with polymer matrix results in the enhancement of mechanical properties such as tensile strength and storage modulus. This improvement in the mechanical properties occurs mainly due to the electrostatic interaction between the various functional groups in polymer and graphene. The parameters like molecular weight, hydrophobicity and polarity also affects the interaction in polymer-graphene nanocomposites.

Recently, polyaniline (PANI), an organic conducting polymer has attracted much attention as one of the promising materials for photocatalytic applications because of its high stability, ease of synthesis, electrical and photoelectrical properties.[64] PANI possesses a delocalized structure composed of benzenoid and quinonoid structural units, which indicate the high mobility of charge carriers upon visible light excitation.[64] Hence, many efforts have been devoted by researchers to design PANI based multicomponent nanocomposites with excellent performance for various technological applications.[65-68] In this regard, Shin et al. [64] prepared PANI-graphene nanocomposites by *in-situ* polymerization of aniline using ammonium peroxydisulphate (APS) as initiator and utilized as efficient photocatalyst for removal of rose bengal (RB) dye form water. RB removal from water is of great significance because of its harmful effects on liver and stomach. It has been investigated with the help of Fourier transform infrared spectroscopy (FTIR) and x-ray

photoelectron spectroscopy (XPS) that hydrogen bonding interactions exist between O=C-O$^-$ group of functionalized graphene and –NH group of PANI during polymerization process. The nanocomposite with 3 wt% of graphene in PANI offers well dispersion of the catalyst and high surface area, which results in better photocatalytic activity as compared to bare PANI, graphene and other nanocomposites with different contents of graphene. The high surface area of PANI-graphene nanocomposites possess high ability of RB dye adsorption due to existence of $\pi \rightarrow \pi^*$ stacking between RB molecules and aromatic groups of graphene. On light illumination, photogenerated charge carriers formation takes place in PANI and presence of graphene in nanocomposite facilitate electron-hole separation. Photogenerated electron-hole separation is followed by transfer of electrons form PANI to graphene, wherein they react with dissolved oxygen and results in the formation of active radical species in the form of O_2^{-*} and OH^* on the catalyst surface. These oxidizing species have potential to mineralize pollutants into CO_2 and H_2O. The schematic illustration of enhanced charge transfer over PANI-graphene nanocomposite to degrade RB dye is shown in **Figure 7**.

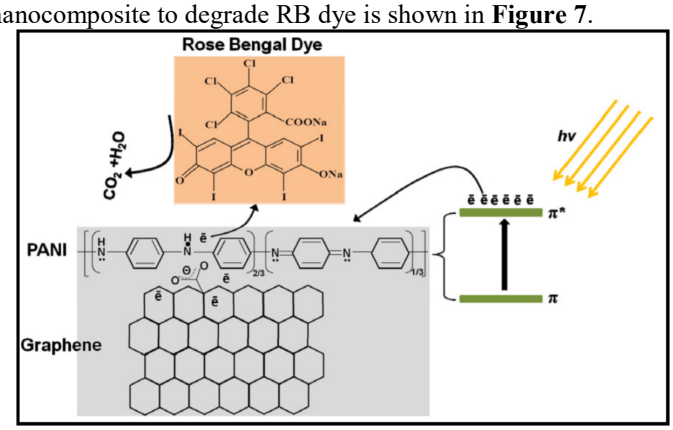

Figure 7. Schematic illustrations of enhanced charge transfer to degrade RB dye over the surface of PANI–graphene nanocomposites. Reprinted with permission from reference [64], copyright 2012 Elsevier.

In addition to this, polyvinyl alcohol (PVA) also demonstrated as promising biocompatible and non-toxic polymers.[69] It is hydrophilic in nature with excellent thermal and chemical stability. PVA can react with various kinds of cross linking agents to form gels, which are highly useful material to be in medical, cosmetic and food industries.[69] The interesting properties of PVA has also been utilized very recently in photocatalytic applications by Zhang et al.[69] who reported nanocomposites composed of 3D graphene oxide-PVA-TiO_2 microspheres for photocatalytic environmental remediation applications by removing methylene blue and methyl violet from water under simulated solar light. The PVA serves as excellent polymeric matrix for dye adsorption by hydrogen bonding interactions between them. Under simulated solar light irradiation for 120 min, the best graphene oxide-PVA-TiO_2 nanocomposites removes more than 90% of the dyes from water, which was many folds higher than bare samples. Thus the abundant reac-

tion sites provided by graphene oxide-PVA interactions with high pollutant adsorption capacity results in excellent photocatalytic performance of the nanocomposites. The excellent pollutant adsorption ability of graphene oxide-polymer nanocomposites has been investigated by Han et al.[70], wherein they reported 3D porous graphene oxide-polyethylenimine (PEI) nanocomposite. This highly porous nanocomposite was found to exhibit high specific surface area of 476 m^2 g^{-1} and shows excellent adsorption capacity for amaranth and orange G (acidic dyes) adsorption. Therefore, such polymer nanocomposites with graphene oxide with high pollutant adsorption can be exploited as efficient photocatalysts for environmental remediation applications

In the past decade, the fabrication of GO assisted free standing membranes has gained much importance and potentially applied for desalination and water purification.[71] Desalination is one of the promising methods of removing salt from water to obtain fresh water which contains less than 1000 mg L^{-1} of total dissolved solids.[72] Thus with increasing population and industrialization, the demand for fresh water has increased globally. Desalination involves the removal of salt by thermal process or membrane process. Membrane based desalination involves reverse osmosis (RO), nanofiltration (NF) and electrodialysis (ED).[73, 74] ED membranes operate under an electric current that causes ions movement through the membranes, while the use of NF membranes have been successfully used to remove divalent ions, such as Ca^{2+} and Mg^{2+} that contribute to water hardness. But NF membranes' desalination suffer from limitation of low efficiency and not effective in reducing the salinity to drinking water standards. However, RO membranes, can actively remove monovalent ions, such as Na^{+} and Cl^{-}. Furthermore, the performance of the membranes is drastically decreased by membrane fouling, which is one of the major concerns in water desalination technology.[71] Since the discovery of graphene in 2004, it has been explored extensively by scientific community for diverse technological applications due to its fascinating electrical and optical properties. Various research groups have successfully employed graphene in desalination application by introducing nanopores in graphene structure.[75, 76] First report on the use of GO incorporated membrane came in 2012 by Geim et al. [77], wherein they fabricated a sub-micrometer thick membrane of GO that allows the permeation of water molecules. Following this, various studies were successfully carried out based on GO incorporated membranes for nanofiltration and ultrafiltration [78, 79]. Moreover, performance of GO based membranes was significantly improved by surface modification with polymers to form composites. In this regard, Kim et al. designed a membrane using layer-by-layer assembly method to form GO nanosheets deposited on the surface of amino polyether sulfone. This membrane was employed as RO membrane and showed much better resistance to chlorine and improved antifouling properties. In another report by Hung et al. [80] polyacrylonitrile (PAN) was used and a membrane with GO was designed by pressure assisted self-assembly method. These membranes were exhibited remarkably improved performance with 99.5 % water recovery, which was attributed to the perfect packing of GO over PAN surface to form composite film.

Recent photocatalyst development on graphene oxide based composites were enlisted in Table 1.

Table 1. Photocatalytic degradation of various pollutants in aqueous solution by graphene based nanocomposites.

Photocata-lysts	Light source	Pollutant con-centration	$t_{completion}$ (min)	Ref. (year)
P25-GR	100 W Hg lamp	MB (2.7 x 10^{-5} M)	55 min	[81] (2010)
P25-GO	20 W lamp	MB (2.5 x 10^{-5} M)	60 min	[82] (2011)
TiO_2-GR	350 W Xe lamp	RhB (5.3 x 10^{-3} mM)	~200 min	[12] (2011)
TiO_2-GR	6 W UV lamp	MB (0.02 g L^{-1})	>80 min	[83] (2011)
TiO_2-GO	1000 W Xe lamp	MO (12 mg L^{-1})	180 min (~40%)	[84] (2010)
TiO_2-GO	20 W UV lamp	MO (10 mg L^{-1})	9 min	[22] (2011)
TiO_2-GO	11 W UV lamp	AO 7 (100 ppm) (Acid orange)	30 min	[85] (2011)
ZnO-GR	8 W UV lamp	MB (1.0 x 10^{-5} M)	40 min	[86] (2011)
ZnO-GR	300 W Hg lamp	RhB (1.0 x 10^{-5} M)	90 min	[87] (2011)
ZnO-GR	20 W UV lamp	MB (10 mg L^{-1})	56 min (~75%)	[88] (2012)
ZnO-GR	Helogen lamp	MB (20 mg L^{-1})	90 min	[89] (2013)
ZnS-GR	500 W Hg lamp	MB (15 mg L^{-1})	30 min	[90] (2011)
ZnS-RGO	150 W Xe lamp	MB (6.25 x 10^{-5} M)	60 min (~80%)	[91] (2013)
CdS-RGO	300 W Xe lamp	MB (100 mg L^{-1})	150 min	[92] (2012)
CuS-RGO	500 W Xe lamp	MB (4 mg L^{-1})	~ 120 min	[93] (2012)
$BiVO_4$-GR	500 W Xe lamp	MB (20 mg L^{-1})	~300 min	[94] (2011)
BiOBr-GR	500 W Xe lamp	MO (7.5 mg L^{-1})	140 min (~82%)	[95] (2012)
BiOI-GR	500 W Xe lamp	MO (7.5 mg L^{-1})	240 min	[96] (2013)
WO_3-GR	150 W Xe lamp	MO (25 mg L^{-1})	120 min	[97] (2012)
Ag_3PO_4-RGO	350 W Xe lamp	MO (10 mg L^{-1})	~210 min	[98] (2013)
Bi_2WO_6-RGO	Helogen	MB (15 mg L^{-1})	90 min	[99] (2013)

	lamp			
Bi_2O_3-RGO	400 W halogen lamp	MB (5.0 mg L^{-1})	240 min	[100] (2013)
MoS_2-RGO	5 W LED	MB (60 mg L^{-1})	60 min	[101] (2014)
SnS_2-RGO	500 W Xe lamp	Rh B (10 mg L^{-1})	120 min	[102] (2013)
TiO_2-ZnO-RGO	300 W Xe lamp	MB (0.3 mg L^{-1})	120 min	[103] (2015)
CdS-ZnO-RGO	Sunlight	MO (1.0 x 10^{-5} M)	60 min	[18] (2016)
RGO–Ag–Bi_2MoO_6	300 W halogen lamp	Phenol (10 mg L^{-1})	300 min	[104] (2016)
ZnO-MoS_2-RGO	Sunlight	MB (5.0 x 10^{-5} M)	60 min	[105] (2016)
ZnO-Ag-RGO	300 W Xe lamp	Rh B (10 mg L^{-1})	~60 min	[106] (2017)
TiO_2-$BiVO_4$-GR	500 W halogen lamp	MB (10 ppm)	10 min	[107] (2017)
TiO_2-Zr-RGO	400 W Hg lamp	EB	90 min	[108] (2017)
TiO_2-RGO	160 W Hg lamp	IB, CM, SM (5.0 mg L^{-1})	~200 min	[109] (2017)
TiO_2-Au-GR	125 W Hg lamp	AB 93 (20 ppm)	120 min (~60 min)	[110] (2017)
CeO_2-GR	400 W Hg lamp	MB	~210 min	[111] (2017)
ZnO-RGO	75 W Xe lamp	RhB, MO, MB (10 mg L^{-1})	~ 300 min	[112] (2017)

GR-graphene; GO-graphene oxide; RGO-reduced graphene oxide; MB-methylene blue; RhB-rhodamine B; MO-methyl orange; EB-eosin blue; IB- ibuprofen; CM- carbamazepine; CM- sulfamethoxazole; AB- acid blue

4 Future perspectives

As discussed above, the graphene and its nanocomposites with semiconductors oxides/ sulfides, metal nanoparticles, carbon quantum dots and polymers have opened up new opportunities in photocatalysis domain. Such heterogeneous photocatalysts offers great advantages, such as cost effectiveness, high efficiency, good thermal stability, tunable band gap structure and facile synthesis routes. Therefore, it has emerged as Green and sustainable approach to remove pollutants

form water by utilizing solar energy. Despite the great achievements over the years with graphene based nanocomposites for pollutants removal, there are still many challenges in fabrication and application of these materials in catalysis. Although various method have been designed and developed for the fabrication of graphene based nanocomposites but still with the increasing demand for high efficiency and optimized parameters, some channelized efforts needs to be carried out in order to achieve large scale practical applications. Therefore, the industrialization of graphene is one of the highly anticipated tasks in coming years as low bulk density can severely hinder its applications. Hence, systematic efforts should be executed to design particular hybrid nanocomposite architectures with desired properties rather than random mixture. Furthermore, it is still challenging to fabricate a cost effective, thin, uniform, high quality graphene layer with controllable layer thickness in nanocomposites, which exhibit distinct electronic, optical and thermal properties.

It is noteworthy to mention here that hybridization of graphene with various polymers have drastically increased the electrical, thermal and mechanical properties of nanocomposites, which display excellent photocatalytic performance to remove the organic pollutants. The strong electronic interactions existing between graphene and conductive polymer matrix provides abundant reaction sites on large specific surface area. Fabrication of devices composed of nanocomposite membranes based on the conductive polymers, graphene and metal oxide/sulfides could be a promising approach to obtain materials with remarkably enhanced photocatalytic performance for pollutants removal form water. Going forward, the utilization of entire solar spectrum is another promising area for graphene based nanocomposites in photocatalysis by exploiting the up-conversion photoluminescence phenomenon of carbon quantum dots and other lanthanide based materials. The development of noble metal free, cost effective nanocomposites which can utilize the near infrared radiation should be further explored in future as it is still not very clear from mechanistic point of view about the up-conversion photoluminescence. Therefore, more studies are required for promoting the general understanding of optical and electronic properties of carbon quantum dots and other up conversion materials.

5 Conclusion

In summary, various graphene based nanocomposites have been designed and demonstrated as efficient heterogeneous photocatalysts for water purification. The introduction of graphene into such nanocomposite have made high impact such as, extended light absorption in visible region, excellent pollutants adsorption, retarded photogenerated electron-hole recombination to prolong their life time, which overall increases the photocatalytic performance as compared to conventional catalysts. In this regard, metal oxide semiconductors, metal nanoparticles and other carbon-based materials have been combined with 2D graphene and widely investigated as nanocomposites with improved charge separation and light

absorption in which graphene acts as excellent support matrix to degrade pollutants from water. Hence collection of all useful properties of 2D graphene, abundance, environmental benignity and facile synthesis routes of its nanocomposites have made it a promising class of functional materials for environmental remediation applications. Unfortunately, despite of all the exciting results obtained so far for pollutant removal with graphene based nanocomposites, this field is still challenges and more efforts needs to be devoted to exploit the graphene based nanocomposites effectively in practical applications. Therefore, in order to maximize the advantages of graphene based nanocomposites, facile and robust synthesis routes should be further developed which can prepare material on large scale to fabricate devices and commercialize them. Moreover, the oxidation of graphite introduces impurities in GO skeleton which leads to decrease in its conductance. The reduction of GO during synthesis to RGO is useful to revive its conductivity, hence the development of highly efficient nanocomposites is still a challenging domain.

Acknowledgements

This work is supported by Sêr Cymru II-Rising Star Fellowship program through Welsh Government and European Regional Development Fund.

References

1. O'Shea, K. E.; Dionysiou, D. D. *The Journal of Physical Chemistry Letters* **2012,** 3, (15), 2112-2113.
2. Deng, Y.; Zhao, R. *Current Pollution Reports* **2015,** 1, (3), 167-176.
3. Chong, M. N.; Jin, B.; Chow, C. W. K.; Saint, C. *Water Research* **2010,** 44, (10), 2997-3027.
4. Dong, S.; Feng, J.; Fan, M.; Pi, Y.; Hu, L.; Han, X.; Liu, M.; Sun, J.; Sun, J. *RSC Advances* **2015,** 5, (19), 14610-14630.
5. Cates, E. L. *Environmental Science & Technology* **2017,** 51, (2), 757-758.
6. Rajeshwar, K.; Thomas, A.; Janáky, C. *The Journal of Physical Chemistry Letters* **2015,** 6, (1), 139-147.
7. Oliver, B. G.; Cosgrove, E. G.; Carey, J. H. *Environmental Science & Technology* **1979,** 13, (9), 1075-1077.

8. Carey, J. H.; Lawrence, J.; Tosine, H. M. *Bulletin of Environmental Contamination and Toxicology* **1976,** 16, (6), 697-701.
9. Frank, S. N.; Bard, A. J. *Journal of the American Chemical Society* **1977,** 99, (1), 303-304.
10. Fujishima, A.; Honda, K. *Nature* **1972,** 238, (5358), 37-38.
11. Ajmal, A.; Majeed, I.; Malik, R. N.; Idriss, H.; Nadeem, M. A. *RSC Advances* **2014,** 4, (70), 37003-37026.
12. Zhang, J.; Xiong, Z.; Zhao, X. *Journal of Materials Chemistry* **2011,** 21, (11), 3634-3640.
13. Kumar, S.; Kumar, A.; Bahuguna, A.; Sharma, V.; Krishnan, V. *Beilstein Journal of Nanotechnology* **2017,** 8, (1), 1571-1600.
14. Zhang, N.; Zhang, Y.; Xu, Y.-J. *Nanoscale* **2012,** 4, (19), 5792-5813.
15. Wang, H.; Zhang, L.; Chen, Z.; Hu, J.; Li, S.; Wang, Z.; Liu, J.; Wang, X. *Chemical Society Reviews* **2014,** 43, (15), 5234-5244.
16. Marschall, R. *Advanced Functional Materials* **2014,** 24, (17), 2421-2440.
17. Han, L.; Wang, P.; Dong, S. *Nanoscale* **2012,** 4, (19), 5814-5825.
18. Kumar, S.; Sharma, R.; Sharma, V.; Harith, G.; Sivakumar, V.; Krishnan, V. *Beilstein Journal of Nanotechnology* **2016,** 7, (1), 1684-1697.
19. Kou, J.; Lu, C.; Wang, J.; Chen, Y.; Xu, Z.; Varma, R. S. *Chemical Reviews* **2017,** 117, (3), 1445-1514.
20. Konstantinou, I. K.; Albanis, T. A. *Applied Catalysis B: Environmental* **2004,** 49, (1), 1-14.
21. Kumar, S. G.; Rao, K. K. *Rsc Advances* **2015,** 5, (5), 3306-3351.
22. Jiang, G.; Lin, Z.; Chen, C.; Zhu, L.; Chang, Q.; Wang, N.; Wei, W.; Tang, H. *Carbon* **2011,** 49, (8), 2693-2701.
23. Zhang, Y.; Tang, Z.-R.; Fu, X.; Xu, Y.-J. *ACS nano* **2010,** 4, (12), 7303-7314.
24. Li, Y.; Xie, W.; Hu, X.; Shen, G.; Zhou, X.; Xiang, Y.; Zhao, X.; Fang, P. *Langmuir* **2009,** 26, (1), 591-597.
25. Bai, X.; Sun, C.; Liu, D.; Luo, X.; Li, D.; Wang, J.; Wang, N.; Chang, X.; Zong, R.; Zhu, Y. *Applied Catalysis B: Environmental* **2017,** 204, 11-20.

26. Lu, Q.; Yu, Y.; Ma, Q.; Chen, B.; Zhang, H. *Advanced Materials* **2016,** 28, (10), 1917-1933.
27. Tan, C.; Zhang, H. *Chemical Society Reviews* **2015,** 44, (9), 2713-2731.
28. Kumar, S.; Sharma, V.; Bhattacharyya, K.; Krishnan, V. *New Journal of Chemistry* **2016,** 40, 5185--5197.
29. Ding, Y.; Zhou, Y.; Nie, W.; Chen, P. *Applied Surface Science* **2015,** 357, 1606-1612.
30. Zhang, L.; Sun, L.; Liu, S.; Huang, Y.; Xu, K.; Ma, F. *Rsc Advances* **2016,** 6, (65), 60318-60326.
31. Jeffery, A. A.; Rao, S. R.; Rajamathi, M. *Carbon* **2017,** 112, 8-16.
32. Ye, A.; Fan, W.; Zhang, Q.; Deng, W.; Wang, Y. *Catalysis Science & Technology* **2012,** 2, (5), 969-978.
33. Li, Q.; Li, X.; Wageh, S.; Al-Ghamdi, A.; Yu, J. *Advanced Energy Materials* **2015,** 5, (14).
34. Chen, Z.; Liu, S.; Yang, M.-Q.; Xu, Y.-J. *ACS applied materials & interfaces* **2013,** 5, (10), 4309-4319.
35. Lim, S. Y.; Shen, W.; Gao, Z. *Chemical Society Reviews* **2015,** 44, (1), 362-381.
36. Li, H.; He, X.; Kang, Z.; Huang, H.; Liu, Y.; Liu, J.; Lian, S.; Tsang, C. H. A.; Yang, X.; Lee, S. T. *Angewandte Chemie International Edition* **2010,** 49, (26), 4430-4434.
37. Xu, X.; Ray, R.; Gu, Y.; Ploehn, H. J.; Gearheart, L.; Raker, K.; Scrivens, W. A. *Journal of the American Chemical Society* **2004,** 126, (40), 12736-12737.
38. Sun, Y.-P.; Zhou, B.; Lin, Y.; Wang, W.; Fernando, K. S.; Pathak, P.; Meziani, M. J.; Harruff, B. A.; Wang, X.; Wang, H. *J. Am. Chem. Soc* **2006,** 128, (24), 7756-7757.
39. Zhang, H.; Huang, H.; Ming, H.; Li, H.; Zhang, L.; Liu, Y.; Kang, Z. *Journal of Materials Chemistry* **2012,** 22, (21), 10501-10506.
40. Yu, B. Y.; Kwak, S.-Y. *Journal of Materials Chemistry* **2012,** 22, (17), 8345-8353.
41. Subramanian, V.; Wolf, E. E.; Kamat, P. V. *Journal of the American Chemical Society* **2004,** 126, (15), 4943-4950.
42. Haes, A. J.; Zou, S.; Schatz, G. C.; Van Duyne, R. P. *The Journal of Physical Chemistry B* **2004,** 108, (1), 109-116.

43. Schider, G.; Krenn, J.; Gotschy, W.; Lamprecht, B.; Ditlbacher, H.; Leitner, A.; Aussenegg, F. *Journal of Applied Physics* **2001,** 90, (8), 3825-3830.
44. Zhou, X.; Liu, G.; Yu, J.; Fan, W. *Journal of Materials Chemistry* **2012,** 22, (40), 21337-21354.
45. Qin, Y.; Li, J.; Kong, Y.; Li, X.; Tao, Y.; Li, S.; Wang, Y. *Nanoscale* **2014,** 6, (3), 1281-1285.
46. Lee, S. J.; Park, G.; Seo, D.; Ka, D.; Kim, S. Y.; Chung, I. S.; Song, H. *Chemistry-A European Journal* **2011,** 17, (30), 8466-8471.
47. Hayakawa, K.; Yoshimura, T.; Esumi, K. *Langmuir* **2003,** 19, (13), 5517-5521.
48. Jain, P. K.; Huang, X.; El-Sayed, I. H.; El-Sayed, M. A. *Accounts of chemical research* **2008,** 41, (12), 1578-1586.
49. Tang, Z.; Shen, S.; Zhuang, J.; Wang, X. *Angewandte Chemie* **2010,** 122, (27), 4707-4711.
50. Ullah, K.; Ye, S.; Zhu, L.; Meng, Z.-D.; Sarkar, S.; Oh, W.-C. *Materials Science and Engineering: B* **2014,** 180, 20-26.
51. Vilian, A. E.; Choe, S. R.; Giribabu, K.; Jang, S.-C.; Roh, C.; Huh, Y. S.; Han, Y.-K. *Journal of Hazardous Materials* **2017,** 333, 54-62.
52. Gallo, A.; Marelli, M.; Psaro, R.; Gombac, V.; Montini, T.; Fornasiero, P.; Pievo, R.; Dal Santo, V. *Green Chemistry* **2012,** 14, (2), 330-333.
53. Tominaga, M.; Shimazoe, T.; Nagashima, M.; Kusuda, H.; Kubo, A.; Kuwahara, Y.; Taniguchi, I. *Journal of Electroanalytical Chemistry* **2006,** 590, (1), 37-46.
54. Zhang, Y.; Zhang, N.; Tang, Z.-R.; Xu, Y.-J. *The Journal of Physical Chemistry C* **2014,** 118, (10), 5299-5308.
55. Ye, W.; Yu, J.; Zhou, Y.; Gao, D.; Wang, D.; Wang, C.; Xue, D. *Applied Catalysis B: Environmental* **2016,** 181, 371-378.
56. Kuilla, T.; Bhadra, S.; Yao, D.; Kim, N. H.; Bose, S.; Lee, J. H. *Progress in polymer science* **2010,** 35, (11), 1350-1375.
57. Ganguli, S.; Roy, A. K.; Anderson, D. P. *Carbon* **2008,** 46, (5), 806-817.
58. Jang, J. Y.; Kim, M. S.; Jeong, H. M.; Shin, C. M. *Composites Science and Technology* **2009,** 69, (2), 186-191.
59. Kalaitzidou, K.; Fukushima, H.; Drzal, L. T. *Carbon* **2007,** 45, (7), 1446-1452.

60. Zheng, W.; Lu, X.; Wong, S. C. *Journal of Applied Polymer Science* **2004,** 91, (5), 2781-2788.
61. Pan, Y. X.; Yu, Z. Z.; Ou, Y. C.; Hu, G. H. *Journal of Polymer Science Part B: Polymer Physics* **2000,** 38, (12), 1626-1633.
62. Du, X.; Xiao, M.; Meng, Y. *European Polymer Journal* **2004,** 40, (7), 1489-1493.
63. Cho, D.; Lee, S.; Yang, G.; Fukushima, H.; Drzal, L. T. *Macromolecular Materials and Engineering* **2005,** 290, (3), 179-187.
64. Ameen, S.; Seo, H.-K.; Akhtar, M. S.; Shin, H. S. *Chemical engineering journal* **2012,** 210, 220-228.
65. Murugan, A. V.; Muraliganth, T.; Manthiram, A. *Chemistry of Materials* **2009,** 21, (21), 5004-5006.
66. Deshpande, N.; Gudage, Y.; Sharma, R.; Vyas, J.; Kim, J.; Lee, Y. *Sensors and Actuators B: Chemical* **2009,** 138, (1), 76-84.
67. Li, Z.-F.; Zhang, H.; Liu, Q.; Sun, L.; Stanciu, L.; Xie, J. *ACS applied materials & interfaces* **2013,** 5, (7), 2685-2691.
68. Li, X.; Wang, D.; Cheng, G.; Luo, Q.; An, J.; Wang, Y. *Applied Catalysis B: Environmental* **2008,** 81, (3), 267-273.
69. Wang, M.; Cai, L.; Jin, Q.; Zhang, H.; Fang, S.; Qu, X.; Zhang, Z.; Zhang, Q. *Separation and Purification Technology* **2017,** 172, 217-226.
70. Sui, Z.-Y.; Cui, Y.; Zhu, J.-H.; Han, B.-H. *ACS applied materials & interfaces* **2013,** 5, (18), 9172-9179.
71. Roberts, D. A.; Johnston, E. L.; Knott, N. A. *water research* **2010,** 44, (18), 5117-5128.
72. Hegab, H. M.; Zou, L. *Journal of Membrane Science* **2015,** 484, 95-106.
73. Van der Bruggen, B.; Vandecasteele, C. *Environmental pollution* **2003,** 122, (3), 435-445.
74. Greenlee, L. F.; Lawler, D. F.; Freeman, B. D.; Marrot, B.; Moulin, P. *Water research* **2009,** 43, (9), 2317-2348.
75. Cohen-Tanugi, D.; Grossman, J. C. *Nano letters* **2012,** 12, (7), 3602-3608.
76. Surwade, S. P.; Smirnov, S. N.; Vlassiouk, I. V.; Unocic, R. R.; Veith, G. M.; Dai, S.; Mahurin, S. M. *Nature nanotechnology* **2015,** 10, (5), 459-464.
77. Nair, R.; Wu, H.; Jayaram, P.; Grigorieva, I.; Geim, A. *Science* **2012,** 335, (6067), 442-444.

78. Wang, E. N.; Karnik, R. *Nature nanotechnology* **2012,** 7, (9), 552-554.
79. Qiu, S.; Wu, L.; Pan, X.; Zhang, L.; Chen, H.; Gao, C. *Journal of Membrane Science* **2009,** 342, (1), 165-172.
80. Hung, W.-S.; An, Q.-F.; De Guzman, M.; Lin, H.-Y.; Huang, S.-H.; Liu, W.-R.; Hu, C.-C.; Lee, K.-R.; Lai, J.-Y. *Carbon* **2014,** 68, 670-677.
81. Zhang, H.; Lv, X.; Li, Y.; Wang, Y.; Li, J. *ACS nano* **2009,** 4, (1), 380-386.
82. Nguyen-Phan, T.-D.; Pham, V. H.; Shin, E. W.; Pham, H.-D.; Kim, S.; Chung, J. S.; Kim, E. J.; Hur, S. H. *Chemical Engineering Journal* **2011,** 170, (1), 226-232.
83. Guo, J.; Zhu, S.; Chen, Z.; Li, Y.; Yu, Z.; Liu, Q.; Li, J.; Feng, C.; Zhang, D. *Ultrasonics sonochemistry* **2011,** 18, (5), 1082-1090.
84. Chen, C.; Cai, W.; Long, M.; Zhou, B.; Wu, Y.; Wu, D.; Feng, Y. *Acs Nano* **2010,** 4, (11), 6425-6432.
85. Liu, J.; Liu, L.; Bai, H.; Wang, Y.; Sun, D. D. *Applied Catalysis B: Environmental* **2011,** 106, (1), 76-82.
86. Xu, T.; Zhang, L.; Cheng, H.; Zhu, Y. *Applied Catalysis B: Environmental* **2011,** 101, (3), 382-387.
87. Li, B.; Cao, H. *Journal of Materials Chemistry* **2011,** 21, (10), 3346-3349.
88. Fan, H.; Zhao, X.; Yang, J.; Shan, X.; Yang, L.; Zhang, Y.; Li, X.; Gao, M. *Catalysis Communications* **2012,** 29, 29-34.
89. Ahmad, M.; Ahmed, E.; Hong, Z.; Xu, J.; Khalid, N.; Elhissi, A.; Ahmed, W. *Applied Surface Science* **2013,** 274, 273-281.
90. Hu, H.; Wang, X.; Liu, F.; Wang, J.; Xu, C. *Synthetic Metals* **2011,** 161, (5), 404-410.
91. Sookhakian, M.; Amin, Y.; Basirun, W. *Applied Surface Science* **2013,** 283, 668-677.
92. Wang, X.; Tian, H.; Yang, Y.; Wang, H.; Wang, S.; Zheng, W.; Liu, Y. *Journal of Alloys and Compounds* **2012,** 524, 5-12.
93. Zhang, Y.; Tian, J.; Li, H.; Wang, L.; Qin, X.; Asiri, A. M.; Al-Youbi, A. O.; Sun, X. *Langmuir* **2012,** 28, (35), 12893-12900.
94. Fu, Y.; Sun, X.; Wang, X. *Materials Chemistry and Physics* **2011,** 131, (1), 325-330.

95. Song, S.; Gao, W.; Wang, X.; Li, X.; Liu, D.; Xing, Y.; Zhang, H. *Dalton Transactions* **2012,** 41, (34), 10472-10476.
96. Liu, H.; Cao, W.-R.; Su, Y.; Chen, Z.; Wang, Y. *Journal of colloid and interface science* **2013,** 398, 161-167.
97. Zhou, M.; Yan, J.; Cui, P. *Materials Letters* **2012,** 89, 258-261.
98. Dong, P.; Wang, Y.; Cao, B.; Xin, S.; Guo, L.; Zhang, J.; Li, F. *Applied Catalysis B: Environmental* **2013,** 132, 45-53.
99. Xu, J.; Ao, Y.; Chen, M. *Materials Letters* **2013,** 92, 126-128.
100. Liu, X.; Pan, L.; Lv, T.; Sun, Z.; Sun, C. Q. *Journal of colloid and interface science* **2013,** 408, 145-150.
101. Li, J.; Liu, X.; Pan, L.; Qin, W.; Chen, T.; Sun, Z. *RSC Advances* **2014,** 4, (19), 9647-9651.
102. Chen, P.; Su, Y.; Liu, H.; Wang, Y. *ACS applied materials & interfaces* **2013,** 5, (22), 12073-12082.
103. Raghavan, N.; Thangavel, S.; Venugopal, G. *Materials Science in Semiconductor Processing* **2015,** 30, 321-329.
104. Meng, X.; Zhang, Z. *Journal of Catalysis* **2016,** 344, 616-630.
105. Kumar, S.; Sharma, V.; Bhattacharyya, K.; Krishnan, V. *New Journal of Chemistry* **2016,** 40, (6), 5185-5197.
106. Surendran, D. K.; Xavier, M. M.; Viswanathan, V. P.; Mathew, S. *Environmental Science and Pollution Research* **2017**, 1-9.
107. Nanakkal, A.; Alexander, L. *Journal of Materials Science* **2017,** 52, (13), 7997-8006.
108. Prabhakarrao, N.; Chandra, M. R.; Rao, T. S. *Journal of Alloys and Compounds* **2017,** 694, 596-606.
109. Lin, L.; Wang, H.; Xu, P. *Chemical Engineering Journal* **2017,** 310, 389-398.
110. Ghasemi, S.; Hashemian, S.; Alamolhoda, A.; Gocheva, I.; Setayesh, S. R. *Materials Research Bulletin* **2017,** 87, 40-47.
111. Khan, M. E.; Khan, M. M.; Cho, M. H. *Scientific Reports* **2017,** 7.
112. Ranjith, K. S.; Manivel, P.; Rajendrakumar, R. T.; Uyar, T. *Chemical Engineering Journal* **2017,** 325, 588-600.